

# 130 MM APERTURE QUADRUPOLES FOR THE LHC LUMINOSITY UPGRADE

F. Borgnolutti, E. Todesco, CERN, Geneva, Switzerland  
A. Mailfert, Nancy Université, LEM, UMR 7569 CNRS-INPL, France

## Abstract

Several studies for the LHC luminosity upgrade pointed out the need for low-beta quadrupoles with apertures larger than the present baseline (70 mm). In this paper we focus on the design issues of a 130 mm aperture quadrupole. We first consider the Nb-Ti option, presenting a magnetic design with the LHC dipole and quadrupole cables. We study the electromagnetic forces and we discuss the field quality constraints. For the Nb<sub>3</sub>Sn option, we sketch three designs, two based on the LARP 10 mm width cable, and one on a larger cable with the same strand. The issue of the stress induced by the e.m. forces, which is critical for the Nb<sub>3</sub>Sn, is discussed using both scaling laws and finite element models.

## INTRODUCTION

The low- $\beta$  insertion in the interaction region of the Large Hadron Collider (LHC) consists of a triplet of superconducting quadrupoles [1] to focus the beam in the interaction point (IP). In the baseline, the value of the beta function in the IP is  $\beta^* = 0.55$  m. Several studies about how to decrease  $\beta^*$  to values of 0.25 m or even less have been carried out [2-10], and designs for magnets in Nb<sub>3</sub>Sn have been proposed [6,11-13]. Here we focus on a recent proposal [14] of staging the LHC upgrade in two phases, the first one replacing the present triplet in Nb-Ti with a 30% longer triplet of the same material, with a nearly double aperture (130 mm instead of 70 mm). We provide a magnet design for this option. This design also satisfies the requirements of the Q2 and Q3 magnets of the “small  $\beta$ -max” lay-out proposed in [15].

A phase-two upgrade would be based on Nb<sub>3</sub>Sn, giving a more compact triplet, giving the possibility of further reducing  $\beta^*$  by 30% [10], and having a better tolerance to heat deposition. These magnets should have an aperture of the order of 130 mm or more [16], i.e. larger than the present baseline of 90 mm established for the LHC Accelerator Research Program [11-13]. In the second part of the paper we address some of the critical issues related to the design of Nb<sub>3</sub>Sn magnets with 130 mm aperture.

## Nb-Ti QUADRUPOLE FOR THE PHASE-ONE UPGRADE

The requirements on the aperture, gradient and length of the quadrupoles are given by the constraints of the optics [10]. Here, we aim at reaching a  $\beta$  function in the IP of 25 cm, and to have 6 additional sigma (in diameter) to reduce the impedance due to the collimators [14,16]. Coupling these requirements with the gradient vs aperture constraint induced by the Nb-Ti technology, we obtain a triplet made up of four magnets “MQXC”. Q1, Q2a, Q2b

and Q3 have the same aperture of 130 mm, and two different lengths, i.e. 9.2 m for Q1-Q3, and 7.8 m for Q2a-Q2b. The required operational gradient is 122 T/m [14]. The proposed cross-section is based on a two layer graded coil, the inner layer being made with the LHC dipole inner cable, and the outer with the LHC main quadrupole cable. The ratio between the cable cross-sections is 1.26, and since the two layers are in series, the current density in the outer layer is 26% higher than in the inner one. Based on the measurements relative to the production of the LHC cables [17], we assume a critical current density

$$j_c(B) = c(B_{c2}^* - B) \quad B < B_{c2}^* \quad (1)$$

with  $c \sim 670$  A/mm<sup>2</sup> and  $B_{c2}^* = 13.5$  T at 1.9 K. This is  $\sim 10\%$  better of what is usually assumed for the Nb-Ti.

Field quality is optimized based on the lay-out of a 33.6° coil with a wedge between 21.6° and 26.1° for the inner layer (setting  $b_6$ ,  $b_{10}$  and  $b_{14}$  to zero), and on a 30° coil for the outer layer (see Fig. 1). Due to the large aperture, the cable key-stoning is enough to have a whole block in the outer layer without requiring an additional wedge to keep the cables in the radial direction.

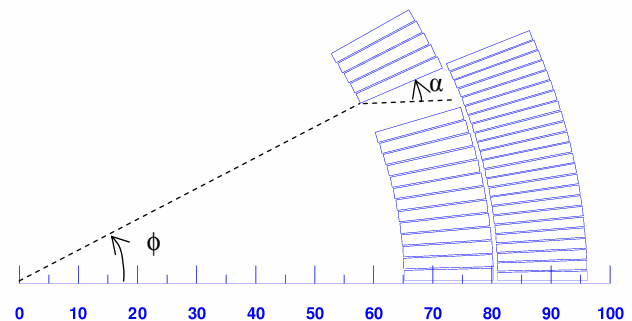


Figure 1: Cross-section proposed for the MQXC

A double mid-plane shim of 0.75 mm (three sheets of 0.125 mm for each quarter) is put in the mid-plane to allow a fine tuning of multipoles during the prototype phase, following the experiences of RHIC [18] and LHC. The position of the blocks is given in Table 1.

Table 1: Position of the coil blocks in MQXC

Block	n cond	$r$ [mm]	$\phi$ [degree]	$\alpha$ [degree]
1	13	65.000	0.331	0.000
2	5	65.000	27.580	23.050
3	24	80.900	0.266	0.000

Collar thickness is assumed to be 25 mm, and iron thickness of 150 mm. Based on this cross-section and on

the critical surface data, the short sample gradient at 1.9 K is estimated to be 148 T/m, and the short sample current 15400 A (without considering the self-field of the strand). This provides a 20% margin for the operational conditions, i.e. 122 T/m and 12300 A. The peak field at operational current is 8.7 T.

Field quality is optimized at operational current rather than at injection since these magnets affect the beam only in the collision optics. The peak field in the iron is 4.2 T, giving a strong saturation, reducing the transfer function in operational conditions of 4.4%. This is similar to what found for the MQXA (6%) and MQXB (2%) [19,20]. The saturation impact on  $b_6$  is  $\sim 3$  units, using a reference radius of 1/3 of the magnet aperture. The geometric component has been used to compensate the saturation. The impact of the iron on  $b_{10}$  and  $b_{14}$  is less than 0.1 units. The design harmonics at nominal gradient of the lay-out shown in Fig. 1 and Table 1 are within one unit.

The inductance per meter (iron included, at operational current using definitions implemented in Roxie [21]) is 7.34 mH/m, and the total inductance is 67.5 mH for the 9.2 m magnet. The stored energy at operational field is 5.1 MJ, i.e. in between the values for the double aperture LHC main dipole (6.9 MJ) and the MQXA values (see Table 2). A preliminary analysis of the protection issue has shown that quench heaters are necessary, and should be fired within 0.1 ms after the quench [22].

Table 2: Features of the inner triplet LHC superconducting quadrupoles, and MQXC design values

	Unit	MQXA	MQXB	MQXC
Aperture	mm	70	70	130
Layers		4	2	2
Operational current	kA	7.15	11.95	12.27
Operational margin	%	20	16	20
Peak field	T	8.6	7.7	8.7
Gradient	T/m	215	215	122
Energy	MJ	2.3	1.3	5.1
Peak stress	MPa	62	44	70

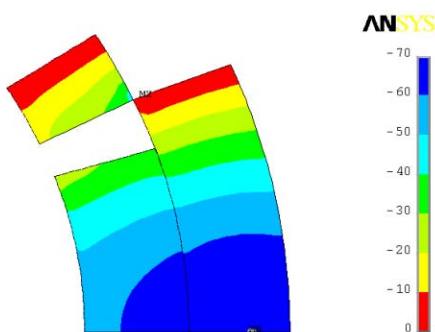


Figure 2: Stress (MPa) induced by electromagnetic forces at nominal current in the Nb-Ti MQXC.

The stress induced by electromagnetic forces at nominal current has been evaluated with a FEM model (see Fig. 2), in the hypothesis of a perfect sliding between the two layers and infinitely rigid collars. The total radial force applied in the mid-plane on each quarter of coil is

2.8 MN/m. The maximal azimuthal stress occurring at the coil mid-plane is 70 MPa, i.e.  $\sim 10\%$  more than MQXA (see Table 2).

## LARGE APERTURE Nb<sub>3</sub>Sn QUADS

A phase-two upgrade should rely on apertures of at least 130 mm diameter, and possibly 145-150 mm [16]. Here, we present Nb<sub>3</sub>Sn quadrupole designs with a 130 mm aperture. We first consider a quadrupole made with either two or four layers (see Fig. 3, left) using the 10mm width cable used for the LARP program [11]. Then we also analyse the case of a two layers coil based on a cable with the same strand but a larger width of 15 mm (see Fig. 3, right). We assume a  $j_{non-cu}$  of 3000 A/mm<sup>2</sup> at 12T and 4.2K corresponding to an upper limit for Nb<sub>3</sub>Sn cabled strands with the present technology.

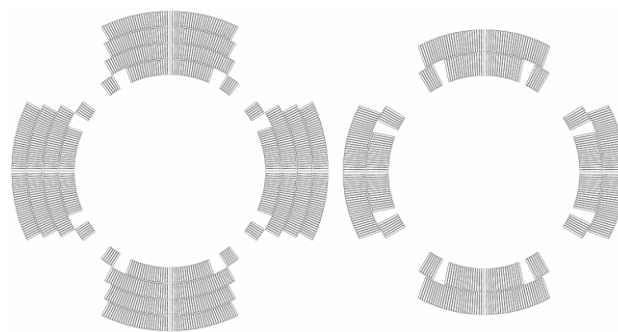


Figure 3: Cross-sections of Nb<sub>3</sub>Sn quadrupoles with four 10 mm (left) and two layers 15 mm (right) wide cable.

Also in this case, the collar thickness is assumed to be 25 mm. Coil geometry has been optimized in order to keep  $b_6$  and  $b_{10}$  within one unit at operational current, taking into account of iron saturation. The reference radius is 1/3 of the magnet aperture.

Quadrupole nominal parameters have been taken with 20% margin of the short sample current and assuming no cable performance degradation (see Table 3). One can reach nominal gradients ranging from 147 To 173 T/m. The stored energy of the four layers lay-out is 50%-100% higher than the two layer cases. We also give an estimate of the magnetic length of the quadrupoles needed in each case, based on the analysis done in [10,14].

Table 3: Parameters of 3 designs of Nb<sub>3</sub>Sn quadrupoles

	Unit	2 Layers	2 Layers	4 Layers
Cable width	mm	10	15	10
Op. current	kA	11.0	13.1	7.6
Peak field	T	10.8	11.8	12.4
Gradient	T/m	147	160	173
Energy	MJ	4.6/5.2	6.2/7.0	8.6/9.7
Quad. length	m	7.0/8.0	6.5/7.4	6.2/7.0

Electromagnetic forces are a crucial issue for Nb<sub>3</sub>Sn magnets, since the cable performances are reduced when the domain of 150-200 MPa of stress is reached [23]. In

order to have an insight on the dependence of stress on the coil width and gradient, an analytical formula [24] has been first used

$$\sigma_{\phi} = -\frac{\sqrt{3}}{8\pi} j_{op}^2 \mu_o \text{Max}_{\rho} \frac{1}{\rho^2} \left[ \rho^4 - r^4 + 4\rho^4 \ln\left(\frac{r+w}{\rho}\right) \right] \quad (3)$$

where  $j_{op}$  is the operational current density in the insulated cable,  $r$  is the aperture radius,  $w$  is the coil width and the maximum has to be taken in  $[r, r+w]$ . In Fig. 4, the stress has been computed for coil widths ranging from 1 to 200 mm (solid line), and in particular for the widths of the three designs (empty markers). The curve shows that in the region of interest the stress is weakly depending on the coil width, i.e. on the operational gradient. The finite element model results (filled markers), in the hypothesis of glued layers (except a perfect sliding between 2<sup>nd</sup> and 3<sup>rd</sup> layers) and infinitely rigid collars, show an agreement within 15%. The actual values are between 120 MPa and 135 MPa, which should not provoke cable degradation at operational current. On the other hand, the short sample current would produce a 56% larger stress, i.e., well beyond the degradation limit.

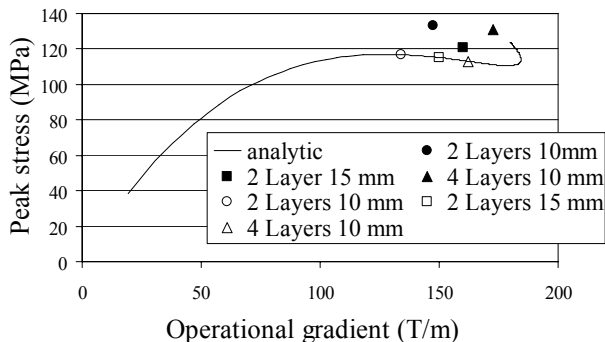


Figure 4: Stress induced by e.m. forces versus gradient at operational current for a 130 mm aperture quadrupole: analytical approximation for a continuous scan over the coil width (solid line), and for 3 magnet designs (empty markers) and FEM values (full markers).

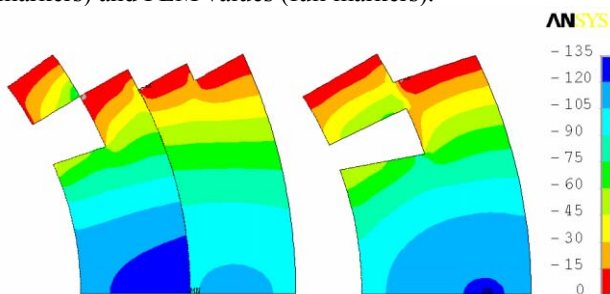


Figure 5: Azimuthal stress (MPa) at operational currents for 10mm cable, 4 layers (left) and 15mm cable, 2 layers.

## CONCLUSIONS

We outlined the electro-magnetic designs of 130 mm

aperture quadrupoles for the LHC low- $\beta$  insertion. A magnet providing 122 T/m operational gradient can be built with a two-layer coil based on the Nb-Ti cables used for the main LHC dipole and quadrupole. The field quality optimization and the impact of the iron saturation are outlined. The pre-stress induced by electromagnetic forces and the aspect related to quench protection (for a 9.2 m long magnet as required by the optics) are shown to be not far from the baseline.

We then analyse the case of a 130 mm aperture Nb<sub>3</sub>Sn quadrupole. Using the LARP cable of 10 mm width we showed that in case of a very good conductor bearing 3000 A/mm<sup>2</sup> at 12 T and 4.2 K, one gets an operational gradient of 147 T/m with a double layer, and 173 T/m with a four layer design. The stress induced by the electromagnetic forces weakly depends on the coil width. The stress at operational current is around 130 MPa, which is still a safe value to avoid cable degradation due to strain.

## REFERENCES

- [1] AA. VV. "LHC Design Report", CERN **2004-003** (2004) pp 32, 47-53, 237-41.
- [2] O. Bruning, et.al., *LHC Project Report* **626** (2002).
- [3] T. Sen, et al., *EPAC* (2002) 371-3.
- [4] J. Strait, et al., *PAC* (2003) 42-5.
- [5] F. Ruggiero, et al., *EPAC* (2004) 608-10.
- [6] R. Ostojic, et al., *PAC* (2005) 2795-7.
- [7] J.P. Koutchouk, *LHC Project Report* **973** (2006).
- [8] R. De Maria, O. Bruning, *EPAC* (2006) 574-6.
- [9] R. De Maria, CARE proceedings, Valencia (2006).
- [10] E. Todesco, J.P. Koutchouk, CARE proceedings, Valencia (2006).
- [11] S. Gourlay, et al, *IEEE Trans. Appl. Supercond.* **16** (2006) 324-7.
- [12] G. Sabbi, et al, *IEEE Trans. Appl. Supercond.* **17** (2007) in press.
- [13] S. Zlobin, et al., PAC03 (2003) 1975-7.
- [14] J.P. Koutchouk, L. Rossi, E. Todesco, *LHC Project Report* **1000** (2007).
- [15] O. Bruning, R. De Maria, R. Ostojic, *LHC Project Report* **1008** (2007).
- [16] J.P. Koutchouk, et al, PAC 2007.
- [17] A. Verweij, A. Gosh, *IEEE Trans. Appl. Supercond.* (2007) in press.
- [18] R.C. Gupta et al., Magnet Technology (MT15) at Beijing, China (1997).
- [19] A. Yamamoto, et al., *IEEE Trans. Appl. Supercond.* **15** (2005) 1084-1089.
- [20] R. Bossart, et al., *IEEE Trans. Appl. Supercond.* **13** (2003) 1297-300
- [21] S. Russenschuck, CERN 99-02 (1999).
- [22] M. Sorbi, E. Todesco, private communication
- [23] E. Barzi, et al., *IEEE Trans. Appl. Supercond.* **15** (2005) 1541-4.
- [24] P. Fessia, et al., *IEEE Trans. Appl. Supercond.* **17** (2007) in press.